# Origin and control of the dominant time constant of salamander cone photoreceptors

Jingjing Zang and Hugh R. Matthews

Physiological Laboratory, Department of Physiology, Development, and Neuroscience, University of Cambridge, Cambridge CB2 3EG, England, UK

Recovery of the light response in vertebrate photoreceptors requires the shutoff of both active intermediates in the phototransduction cascade: the visual pigment and the transducin–phosphodiesterase complex. Whichever intermediate quenches more slowly will dominate photoresponse recovery. In suction pipette recordings from isolated salamander ultraviolet- and blue-sensitive cones, response recovery was delayed, and the dominant time constant slowed when internal $[Ca^{2+}]$ was prevented from changing after a bright flash by exposure to $0Ca^{2+}/0Na^+$ solution. Taken together with a similar prior observation in salamander red-sensitive cones, these observations indicate that the dominance of response recovery by a $Ca^{2+}$-sensitive process is a general feature of amphibian cone phototransduction. Moreover, changes in the external pH also influenced the dominant time constant of red-sensitive cones even when changes in internal $[Ca^{2+}]$ were prevented. Because the cone photopigment is, uniquely, exposed to the external solution, this may represent a direct effect of protons on the equilibrium between its inactive Meta I and active Meta II forms, consistent with the notion that the process dominating recovery of the bright flash response represents quenching of the active Meta II form of the cone photopigment.

## INTRODUCTION

The vertebrate retina operates over a range of intensities that exceeds 12 orders of magnitude. This wide intensity range is enabled, in part, by the possession of two classes of photoreceptor: the rods, which operate at low intensities and are capable of signaling the absorption of single photons, and the cones, which respond more rapidly at considerably higher intensities (Fu and Yau, 2007). Despite the duplex nature of the retina, the less sensitive cones nevertheless have to operate over a nine–order of magnitude intensity range, necessitating considerable adaptation of the sensitivity and kinetics of their responses during steady illumination (Baylor and Hodgkin, 1974; Matthews et al., 1990; Schneeweis and Schnapf, 1999). In both rods and cones, the process of phototransduction involves an enzymatic cascade initiated by the absorption of light by an 11-cis-retinal chromophore covalently associated with a protein opsin to form a G protein–coupled photopigment. The light-activated (Meta II) form of the photopigment interacts with a heterotrimeric G protein (transducin), which in turn activates its target effector enzyme, a phosphodiesterase that hydrolyses cGMP. The ensuing reduction in cGMP concentration leads to the closure of CNG channels in the outer segment membrane, yielding the diminution of the circulating current through these channels in darkness, which constitutes the electrical response to light. The associated reduction in $Ca^{2+}$ influx through the CNG channels is accompanied by continuing $Ca^{2+}$ efflux via $Na^+$-$Ca^{2+}$,$K^+$ exchange, leading to a decrease in the concentration of $Ca^{2+}$ within the outer segment during the photoresponse (Yau and Nakatani, 1985). This light-induced decrease in $[Ca^{2+}]_i$ is crucial to the process of light adaptation (Burns and Baylor, 2001; Fain et al., 2001; Lamb and Pugh, 2006), leading to accelerated cGMP synthesis by guanylyl cyclase (Koch and Stryer, 1988), speeded quenching of activated photopigment by phosphorylation (Kawamura, 1993), and increased cGMP affinity of the CNG channel (Hsu and Molday, 1993).

To terminate the light response and restore the dark-adapted sensitivity, all of the intermediates in the transduction cascade must be quenched, and the cGMP concentration must be restored. The translational invariance of the recovery of the responses to saturating flashes of increasing intensity has been taken as indicating that response recovery is governed by a single dominant time constant, which is believed to represent the slowest of these quenching processes (Hodgkin and Nunn, 1988; Nikonov et al., 1998; Pepperberg et al., 1992). However, the molecular nature of the rate-limiting step underlying the dominant time constant remains controversial and may differ between rods and cones. In rods, Meta II rhodopsin is quenched by its $Ca^{2+}$-dependent phosphorylation (Bownds et al., 1972; Kühn

and Dreyer, 1972), followed by the binding of arrestin (Kühn et al., 1984). In contrast, shutoff of transducin results from its intrinsic GTPase activity (Arshavsky and Bownds, 1992), which is not believed to depend on $Ca^{2+}$. Whichever of these processes takes place the most slowly will dominate the ultimate recovery of the photoresponse. In amphibian rods, the time constant that normally dominates the recovery of the saturating flash response does not appear to depend on $Ca^{2+}$ (Lyubarsky et al., 1996; Matthews, 1996), whereas a faster and $Ca^{2+}$-dependent process (Matthews, 1997) can be prolonged to instead dominate response recovery by substituting a modified chromophore that slows Meta II rhodopsin quenching (Matthews et al., 2001). Thus, it would appear that the $Ca^{2+}$-sensitive quenching of rhodopsin does not normally dominate recovery of the amphibian rod saturating photoresponse, suggesting that recovery is instead dominated by the GTPase activity of transducin (Sagoo and Lagnado, 1997). In mammalian rods, however, this question has evoked more controversy (Burns and Pugh, 2010). On the one hand, enhancement of transducin GTPase activity by overexpression of RGS-9 has been shown to accelerate the dominant time constant, suggesting that recovery is dominated by transducin deactivation (Krispel et al., 2006). In contrast, the increased single-photon response variability seen upon reduced expression of arrestin and rhodopsin kinase has been interpreted as suggesting that rhodopsin lifetime might limit response recovery instead (Doan et al., 2009). However, this confusion has recently been resolved by the demonstration in mice in which levels of both arrestin and RGS-9 were modified that both rhodopsin phosphorylation and arrestin binding take place with a time constant of $\sim$40 ms in the wild-type animal (Gross and Burns, 2010), a value sufficiently fast to render photopigment quenching nondominant in mammalian rods also.

Cone phototransduction has been studied in less detail than in rods, leaving open the possibility that, despite the fundamental similarities between their transduction cascades, significant differences might exist in the control of their responses (Fu and Yau, 2007). Recent evidence suggests that this is indeed the case for salamander red-sensitive cones, in which the time constant dominating the recovery of the saturating flash response has been shown to depend on $Ca^{2+}$ and to be speeded by an anion substitution designed to accelerate the quenching of the red cone photopigment (Matthews and Sampath, 2010). These results suggest that photopigment quenching dominates flash response recovery in red-sensitive cones, thereby conferring $Ca^{2+}$ dependence upon their response kinetics during adaptation over the extensive cone operating range. To determine whether this is a general feature of cone phototransduction, we have extended this approach to the other salamander cone spectral classes. In this study, we have investigated the role of $Ca^{2+}$ in modulating the flash response in salamander UV- and blue-sensitive cone photoreceptors. We found in both cases that the flash response remained sensitive to $Ca^{2+}$ for its entire duration and that the dominant time constant for recovery of the response to a saturating flash was prolonged when the $Ca^{2+}$ concentration was not allowed to fall. These results are similar to those obtained in the red-sensitive cone (Matthews and Sampath, 2010) and indicate that the dominance of response recovery by $Ca^{2+}$-sensitive photopigment quenching instead of transducin shutoff is a general feature of amphibian cone phototransduction. Moreover, to study further the molecular identity of the process dominating red-sensitive cone recovery, we investigated the effect on the dominant time constant of protons, which favor the active Meta II form of the photopigment (Parkes and Liebman, 1984). Under conditions where the outer segment $Ca^{2+}$ concentration was maintained at its dark-adapted level, we found that external acidification from the physiological value speeded the dominant time constant, whereas external alkalinisation slowed it, consistent with the notion that protons encourage formation of the active Meta II form of the photopigment whose quenching dominates red-sensitive cone response recovery after a saturating flash. Preliminary results of these findings have been presented to the International Union of Physiological Sciences and the Physiological Society (Zang, J., and H.R. Matthews. 2009. Proceedings of the XXXVI International Congress of Physiological Sciences. Poster P1AM-12-3; Zang, J., and H.R. Matthews. 2010. Proceedings of The Physiological Society. Abstr. C30).

## MATERIALS AND METHODS

### Preparation and external solutions

Details of the preparation, recording techniques, light stimuli, and fast solution changes have been described in detail elsewhere (Matthews, 1995; Matthews and Sampath, 2010) and are presented here briefly. The majority of experiments were performed on cones isolated from the retinae of aquatic tiger salamanders (*Ambystoma tigrinum*; Charles D. Sullivan Co.); experiments on rods instead used land-phase spotted salamanders (*Ambystoma maculatum*; Strictly Reptiles Ltd.). Animals were dark adapted (normally overnight) and then killed under dim red illumination by stunning with a cranial concussion followed by decapitation and pithing according to schedule I of the Animals (Scientific Procedures) Act (1986). Each eyeball was removed and hemisected, and pieces of eyecup were stored in darkness at 4°C until required. Photoreceptors were dissociated mechanically by chopping a piece of isolated retina on a Sylgard (Dow Corning) substrate under infrared illumination. The resulting cell suspension was transferred to the recording chamber on the stage of an inverted microscope (Diaphot; Nikon) and allowed to settle for 10 min before superfusion with amphibian Ringer's solution containing 111 mM NaCl, 2.5 mM KCl, 1 mM $CaCl_2$, 1.6 mM $MgCl_2$, 10 µm EDTA as chelator for heavy metal ions, 10 mM glucose, and 3 mM HEPES buffer, adjusted to pH 7.7–7.8 with NaOH. All experiments were performed at room temperature (20°C).

Changes in $Ca^{2+}$ concentration during the light response were opposed using a $0Ca^{2+}/0Na^+$ solution designed to minimize simultaneously both influx and efflux of calcium across the outer segment membrane (Matthews et al., 1988; Nakatani and Yau, 1988). This solution consisted of 111 mM guanidinium chloride, 2.5 mM KCl, 2 mM EGTA, and 3 mM HEPES buffer, adjusted to pH 7.7 with tetramethylammonium hydroxide. In the complete absence of added $CaCl_2$ and $MgCl_2$, the EGTA buffer served to reduce the free divalent concentrations to extremely low levels (Matthews, 1996). In experiments with modified extracellular pH, the HEPES proton buffer was substituted with an alternative membrane-impermeant "Good"-family buffer (pH 6.6, MOPSO; pH 8.5, EPPS; pH 9.0, CAPSO; Good et al., 1966) titrated to the indicated pH within its buffering range.

### Electrical recording, light stimuli, and fast solution exchange
The inner segment of an isolated photoreceptor was drawn into a suction pipette so that the entire outer segment remained exposed to the superfusing solution. This recording geometry may have resulted in the collection of a smaller fraction of the circulating current than is the case when the outer segment is recorded from directly. Suction pipette currents were filtered using a Bessel low-pass filter (DC-40 Hz for cones and DC-20 Hz for rods) and digitized continuously for subsequent analysis using a PC equipped with an intelligent interface card (Cambridge Research Systems). Figure preparation and curve fitting were performed with Origin (Microcal Software) and QTIplot.

Light flashes of 20-ms duration were delivered from an optical bench via a high-speed electromechanical shutter (Vincent Associates); the light intensity was attenuated by calibrated neutral density filters (Schott). In experiments on cones, the light source was a high-intensity mercury discharge lamp (SUV-DC-E; Lumatec). Visible light stimuli were delivered at nominal wavelengths of 578 nm (red-sensitive cones) and 436 nm (blue-sensitive cones) via narrow band interference filters (Comar Instruments). UV light stimuli (UV-sensitive cones) were delivered via a switchable short-pass filter built into the light source and designed to pass principally the 362-nm mercury line. Cones were assigned to UV-, blue-, and red-sensitive classes on the basis of their sensitivity at these wavelengths, which are close to their respective spectral response maxima (Perry and McNaughton, 1991). In experiments on rods, a tungsten–halogen light source was used to deliver 500-nm stimuli via a narrow band interference filter. These control experiments were performed on the so-called "red rods," which constitute the overwhelming majority in the salamander retina (Hárosi, 1975) and are identified by their characteristic morphology and their sensitivity to 500-nm light. The absolute intensity of light stimuli was measured at the location of the recording chamber with a UV-enhanced silicon photodiode (Centronic) connected to a radiometric optometer (S370; Graseby Optronics), which was also used to calibrate the neutral density filters at each wavelength. In addition, a calibrated infrared blocking filter (KG1; CVI Melles Griot) was used to prevent infrared wavelengths present in the output of the mercury discharge light source in UVA mode from reaching the photodiode during UV calibration.

Rapid solution changes from Ringer's solution to $0Ca^{2+}/0Na^+$ solution were achieved by translating the interface between two rapidly flowing streams of solution across the exposed outer segment using a computer-controlled stepper motor coupled to the microscope stage (Matthews, 1995, 1996). The rapid solution change could be performed in $\sim$50 ms, estimated from the rising phase of the junction current driven by the liquid junction potential between the dissimilar solutions in the suction pipette and bath. Junction currents were obtained by exposing the outer segment to the solution change during steady light of sufficient intensity to completely suppress the circulating current. The timings of solution changes were determined from the half-rise times of the junction current. The outer segment current was obtained by subtracting the junction current from the suction pipette current recorded during the experimental protocol.

## RESULTS

### $Ca^{2+}$ modulates UV- and blue-sensitive cone response recovery
To explore the effect of $Ca^{2+}$ concentration on the time course of response recovery in salamander UV- and blue-sensitive cones, a $0Ca^{2+}/0Na^+$ solution designed to minimize simultaneously both $Ca^{2+}$ influx and efflux (Matthews et al., 1988; Nakatani and Yau, 1988) was used to delay the dynamic fall in $Ca^{2+}$ concentration, which normally accompanies the response to a bright flash (Matthews and Sampath, 2010). Because the outer segment was returned to Ringer's solution while the response remained in saturation, the outer segment $Ca^{2+}$ concentration would then have fallen from near its original dark level to the greatly reduced level established within <200 ms when all the CNG channels are closed (Sampath et al., 1999) before the onset of response recovery. The effect of this manipulation on the timing of response recovery was used to investigate the period over which quenching of the transduction cascade remains sensitive to $Ca^{2+}$ (Matthews, 1997).

This approach is illustrated for a UV-sensitive cone in Fig. 1 A. First, the cone outer segment was stepped into $0Ca^{2+}/0Na^+$ solution; this solution change was accompanied by a negative junction current driven by the liquid junction potential between the guanidinium-substituted solution in the bath and the Ringer's solution in the suction pipette. A bright flash was delivered 1 s later, suppressing the inward dark current carried by guanidinium through the CNG channels of the outer segment membrane. At a variable time thereafter, while the flash response still remained in saturation, the outer segment was returned to normal Ringer's solution, thereby allowing the $Ca^{2+}$ concentration to fall before the onset of response recovery. The recovery phases are replotted in Fig. 1 B after subtraction of the junction current. The time at which the response recovered from saturation by 25% (Fig. 1 B, dashed line) was measured as in previous studies (Matthews, 1997; Matthews and Sampath, 2010) and is plotted in Fig. 1 C as a function of the time spent in $0Ca^{2+}/0Na^+$ solution after the flash. When the flash was delivered in the absence of the solution change (Fig. 1 B, heavy trace), thereby allowing the outer segment $Ca^{2+}$ concentration to fall immediately, the response recovered to the criterion level in just over 2 s. However, when the outer segment was exposed to $0Ca^{2+}/0Na^+$ solution, response recovery was progressively delayed in direct proportion to the time spent in this solution after the flash (Fig. 1 C, solid regression line). The relatively small response amplitude
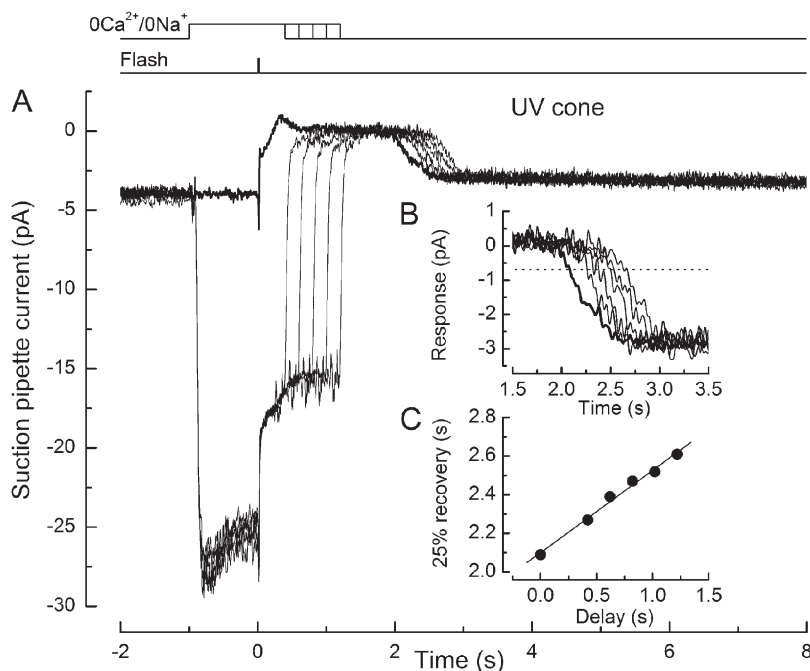
**Figure 1.** Effect on the bright flash response in a salamander UV-sensitive cone of superfusion with $0Ca^{2+}/0Na^+$ solution. (A) Superimposed responses to saturating flashes in Ringer's solution (heavy trace) and upon exposure to $0Ca^{2+}/0Na^+$ solution from 1 s before the flash until progressively increasing times thereafter (light traces). Top traces represent solution change and flash command timings. Suction pipette currents include a junction current resulting from the liquid junction potential between the dissimilar solutions in pipette and bath. Each trace is the mean of two responses; measurements were bracketed symmetrically in time. The bright flash delivered $2.5 \times 10^6$ photons $\mu m^{-2}$ at 362 nm. (B) Recovery phases of the responses from A after subtraction of the junction current obtained on the return to Ringer's solution after a 2-s exposure to $0Ca^{2+}/0Na^+$ solution at the end of the experiment. For each trace, the junction current has been offset in time to coincide with the return to Ringer's solution. Data have been digitally low-pass filtered at 20 Hz. The heavy trace denotes the response in Ringer's solution. (C) Dependence of response duration on the time spent in $0Ca^{2+}/0Na^+$ solution after the flash. Response duration was measured as the time taken after the flash for 25% recovery of current (dashed line in B). Times of the solution changes were measured from the half-relaxation time of the junction current. Regression line of slope 0.43 was fitted using a least-squares algorithm.

seen in this example may reflect, in part, reduced current collection in the outer segment–exposed recording geometry, whereas the early response "peak" seen in this and some other control responses is likely to represent the behavior of voltage-gated conductances in the inner segment membrane within the recording pipette. Equivalent results obtained from a blue-sensitive cone using this protocol are shown in Fig. 2. Again, it can be seen that the time taken for the response to recover to the criterion level increased in direct proportion to the time spent in $0Ca^{2+}/0Na^+$ solution after the flash (Fig. 2 C).

Because the outer segment $Ca^{2+}$ concentration would have fallen rapidly upon the return to Ringer's solution, the progressive delay in response recovery seen when the outer segment was exposed to $0Ca^{2+}/0Na^+$ solution during the period of saturation cannot have resulted from rapid effects of $Ca^{2+}$ on guanylyl cyclase or the CNG channel. Instead, these observations indicate that the transduction cascade remained sensitive to $Ca^{2+}$ for the entire duration of the response in salamander UV- and blue-sensitive cones, as has been shown to be the case for the red-sensitive cones of this species (Matthews and Sampath, 2010), and in dramatic contrast to the situation in salamander rods (Matthews, 1996, 1997).

Collected data from this protocol are shown in Fig. 3 for seven UV-sensitive cones (Fig. 3 A) and six blue-sensitive cones (Fig. 3 B). The increase in the time for 25% recovery when compared with the corresponding control response in Ringer's solution rose linearly with the time spent in $0Ca^{2+}/0Na^+$ solution after the flash with a slope of $0.43 \pm 0.07$ ($\pm$SEM) in UV-sensitive cones and $0.62 \pm 0.05$ in blue-sensitive cones. The linearity of this relationship is consistent with the notion that in UV- and blue-sensitive cones, as in red cones (Matthews and Sampath, 2010), the process that dominates response recovery depends on the outer segment $Ca^{2+}$ concentration, decaying only slowly when $[Ca^{2+}]_i$ is maintained at its initial dark-adapted level and then accelerating once $[Ca^{2+}]_i$ is allowed to fall (Matthews et al., 2001). This simple model would imply, if the solution changes and the concomitant fall in $[Ca^{2+}]_i$ were instantaneous, an acceleration of the time constant dominating recovery by a factor of 1.8 in UV-sensitive and by a factor of 2.6 in blue-sensitive cones (see Fig. 9 and Eq. 2 in Matthews et al., 2001).

### $Ca^{2+}$ controls the dominant time constant of UV- and blue-sensitive cones

The duration of the response to supersaturating flashes is believed to be governed by the dominant time constant for the shutoff of the phototransduction cascade, which can be determined from the slope of the plot relating the time for the response to recover to a criterion level to the natural logarithm of the flash intensity (Pepperberg et al., 1992; Nikonov et al., 1998). This approach, which has been applied previously to salamander red-sensitive
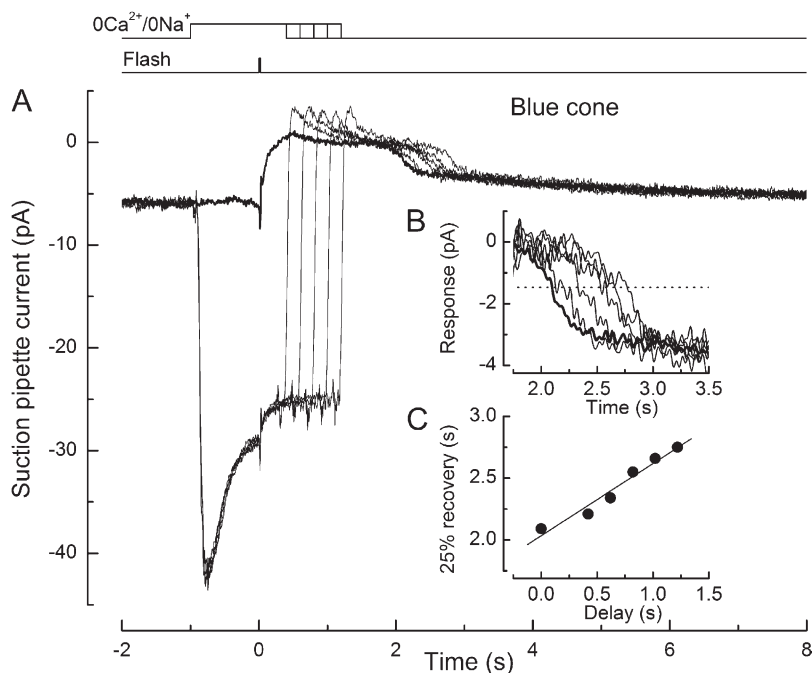
**Figure 2.** Effect on the bright flash response in a salamander blue-sensitive cone of superfusion with $0Ca^{2+}/0Na^+$ solution. (A) Superimposed responses to saturating flashes in Ringer's solution (heavy trace) and upon exposure to $0Ca^{2+}/0Na^+$ solution from 1 s before the flash until progressively increasing times thereafter (light traces). Top traces represent solution change and flash command timings. Suction pipette currents have not been corrected for the junction current. Each trace is the mean of two responses. The bright flash delivered $3.3 \times 10^5$ photons $\mu m^{-2}$ at 436 nm. (B) Recovery phases of the responses from A after subtraction of the junction current as in Fig. 1 B. Data have been digitally low-pass filtered at 20 Hz. The heavy trace denotes the response in Ringer's solution. (C) Dependence of response duration on the time spent in $0Ca^{2+}/0Na^+$ solution after the flash. Response duration was measured as the time taken after the flash for 25% recovery of current (dashed line in B). Regression line of slope 0.58 was fitted using a least-squares algorithm.

cones (Matthews and Sampath, 2010), was used to investigate the effect of $Ca^{2+}$ on the dominant time constant more directly in UV-sensitive (Fig. 4) and blue-sensitive (Fig. 5) cones. Values of the dominant time constant obtained from a series of saturating flashes of increasing intensity delivered in normal Ringer's solution (Figs. 4 A and 5 A), when $[Ca^{2+}]_i$ is free to fall during the response, were compared, in different cells, with values obtained after stepping the outer segment into $0Ca^{2+}/0Na^+$ solution (Figs. 4 B and 5 B), which opposes the light-induced fall in $Ca^{2+}$ concentration (Matthews and Sampath, 2010) and which, in both cases, considerably retarded response recovery as in red-sensitive cones (Nakatani and Yau, 1988; Matthews et al., 1990). These responses were then corrected by the subtraction of junction currents,

and the times for 25% response recovery were measured as in previous figures.

Collected recovery time data obtained under these two conditions from junction current-corrected responses are plotted in Figs. 4 C and 5 C for UV- and blue-sensitive cones, respectively. For both receptor classes, the time for the response to recover to a 25% criterion level varied approximately linearly with the natural logarithm of the flash intensity. The slope of this relationship was relatively shallow in Ringer's solution (Figs. 4 C and 5 C, open circles), when $[Ca^{2+}]_i$ was free to fall during the flash response, yielding values for the dominant time constant of $0.38 \pm 0.05$ s from eight UV-sensitive cones and $0.39 \pm 0.04$ s from 11 blue-sensitive cones. In contrast, the slope of this relationship was increased when
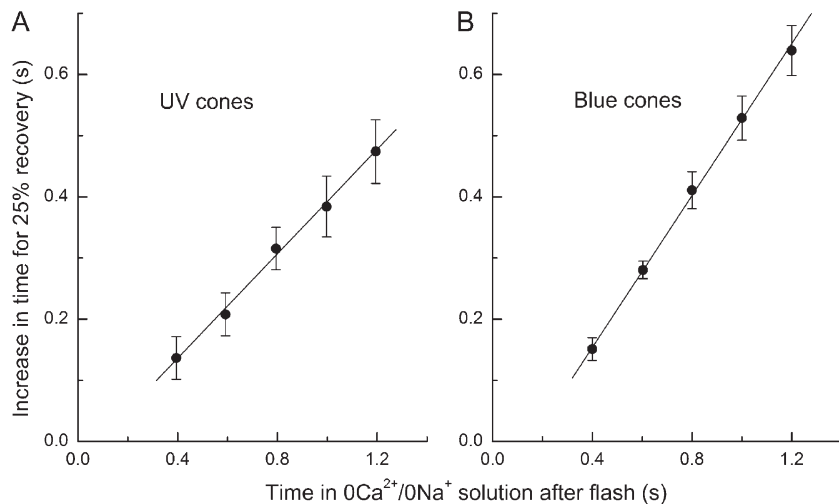


**Figure 3.** Collected data illustrating the dependence of the prolongation of response duration on the time spent in $0Ca^{2+}/0Na^+$ solution after a bright flash as in Figs. 1 and 2. Response prolongation was measured for each cone as the difference between the time taken after the flash for the response to recover by 25% when exposed to $0Ca^{2+}/0Na^+$ solution for the indicated period and the time for 25% recovery of the same cone in Ringer's solution. (A) Mean data from seven UV-sensitive cones, as in Fig. 1; error bars represent SEM. Regression line of slope $0.43 \pm 0.07$ was fitted using a weighted least-squares algorithm. (B) Mean data from six blue-sensitive cones, as in Fig. 2. Regression line of slope $0.62 \pm 0.05$.
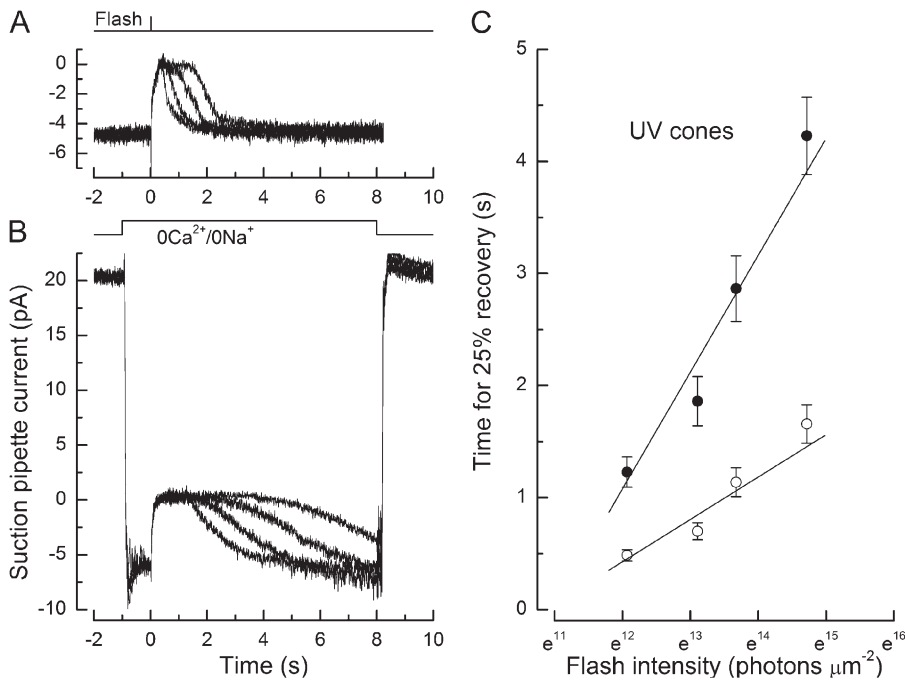
**Figure 4.** Determination of the dominant time constant from the dependence of UV-sensitive cone response duration on supersaturating flash intensity. (A and B) Superimposed suction pipette current recordings of the responses from two representative UV-sensitive cones. (A) Flashes delivered to a UV-sensitive cone in Ringer's solution. (B) Flashes delivered to another UV-sensitive cone in $0Ca^{2+}/0Na^+$ solution, without correction for the junction current. In both cases, the intensity of the 362-nm flashes increased from $1.7 \times 10^5$ to $2.5 \times 10^6$ photons $\mu m^{-2}$. Each trace is the mean of two responses. (C) Mean data for the dependence of response duration on flash intensity in Ringer's solution (protocol as in A; open circles; eight cells) and $0Ca^{2+}/0Na^+$ solution measured after junction current correction (protocol as in B; closed circles; nine cells). Error bars denote SEM. Regression lines of slopes $0.38 \pm 0.05$ s (Ringer's solution) and $1.04 \pm 0.12$ s ($0Ca^{2+}/0Na^+$ solution) were fitted by a weighted least-squares algorithm.

the flash was delivered in $0Ca^{2+}/0Na^+$ solution (Figs. 4 C and 5 C, closed circles), which opposed the dynamic fall in $Ca^{2+}$ concentration during the response, yielding values for the dominant time constant of $1.04 \pm 0.12$ s from nine UV-sensitive cones and $0.80 \pm 0.15$ s from six blue-sensitive cones. These results indicate that when the $Ca^{2+}$ concentration is allowed to fall, the time constant

dominating saturating flash response recovery is accelerated, shortening by 2.7-fold in UV-sensitive and 2.1-fold in blue-sensitive cones when $[Ca^{2+}]_i$ declines from its dark-adapted level to the value during response saturation. This approach to determining the dominant time constant is based on the approximate translational invariance of the recovery of the bright flash response
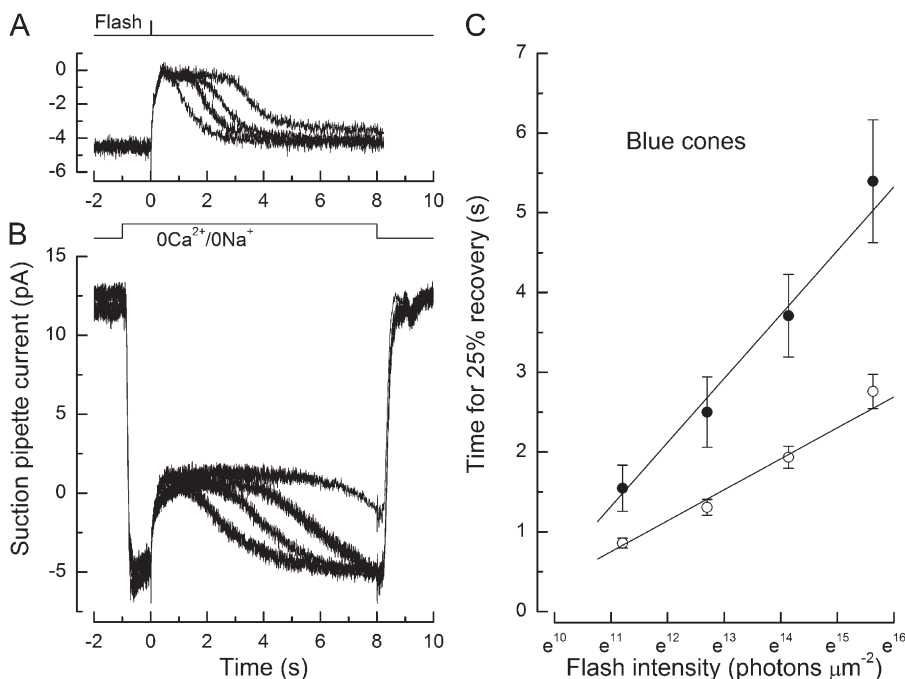


**Figure 5.** Determination of the dominant time constant from the dependence of blue-sensitive cone response duration on supersaturating flash intensity. (A and B) Superimposed suction pipette current recordings of the responses from two representative blue-sensitive cones. (A) Flashes delivered to a blue-sensitive cone in Ringer's solution. (B) Flashes delivered to another blue-sensitive cone in $0Ca^{2+}/0Na^+$ solution without correction for the junction current. In both cases, the intensity of the 436-nm flashes increased from $7.3 \times 10^4$ to $6.1 \times 10^6$ photons $\mu m^{-2}$. Each trace is the mean of two responses. (C) Mean data for the dependence of response duration on flash intensity in Ringer's solution (protocol as in A; open circles; 11 cells) and $0Ca^{2+}/0Na^+$ solution measured after junction current correction (protocol as in B; closed circles; six cells). Error bars denote SEM. Regression lines of slopes $0.39 \pm 0.04$ s (Ringer's solution) and $0.80 \pm 0.15$ s ($0Ca^{2+}/0Na^+$ solution) were fitted by a weighted least-squares algorithm.

(Lyubarsky et al., 1996; Nikonov et al., 1998), which has been illustrated previously in red cones (Matthews and Sampath, 2010). Although it is tempting to interpret further the waveform of response recovery at times after attainment of the 25% recovery criterion, there are potential risks in doing so in $0Ca^{2+}/0Na^{+}$ solution, especially at later times well after recovery from saturation, by when total guanidinium influx may have become significant (Fain et al., 1989) and stability of $Ca^{2+}$ concentration in this solution may have been compromised (Matthews and Fain, 2003). We have therefore not systematically investigated any subtle deviations from translational invariance in these experiments.
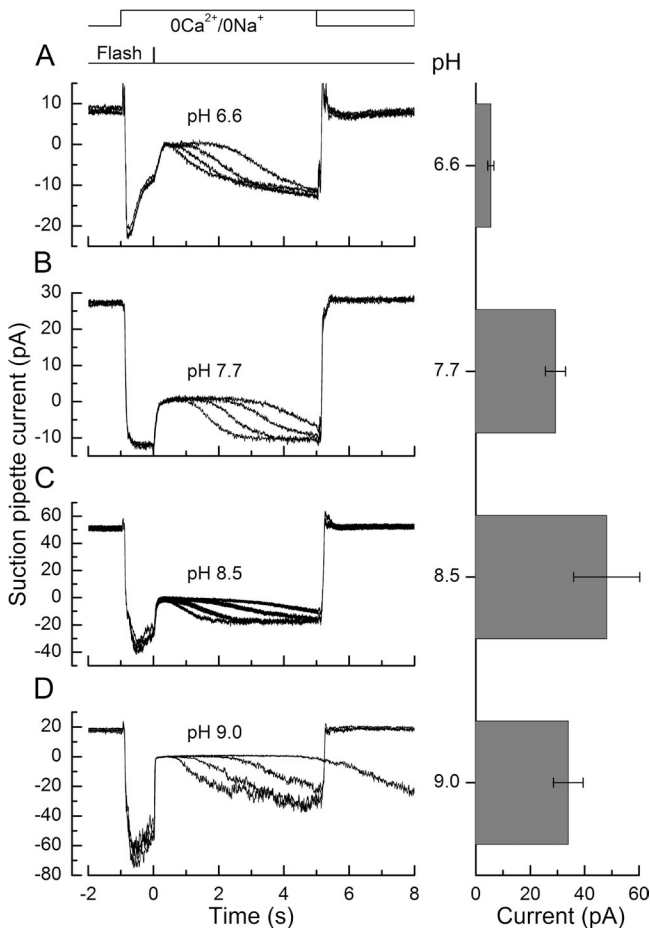


**Figure 6.** Effect of pH on the responses of red-sensitive cones in the absence of light-induced changes in $Ca^{2+}$ concentration. Flashes of increasing intensity were delivered in $0Ca^{2+}/0Na^{+}$ solution buffered to pH 6.6, 7.7, 8.5, and 9.0. The left-hand panels show superimposed suction pipette current recordings of the responses without correction for the junction current from four representative cones. Each trace is the mean of two responses. Top traces represent solution change and flash command timings. Bright flashes at 578 nm were delivered between $1.1 \times 10^{4}$ and $3.6 \times 10^{6}$ photons $\mu m^{-2}$ (also see right-hand panels in Fig. 7). The right-hand panels plot collected data for the mean dark current in each solution (mean ± SEM; data were collected from 9 cones at pH 6.6, 49 cones at pH 7.7, 12 cones at pH 8.5, and 16 cones at pH 9.0).

## The dominant time constant of red-sensitive cones is modulated by pH

In salamander red-sensitive cones, the dominant time constant has been suggested to represent photopigment quenching not only through its dependence on $Ca^{2+}$ concentration (Kawamura, 1993) but also because it can be accelerated by the removal of external chloride ions (Matthews and Sampath, 2010), a manipulation that influences an anion-binding site on the long wavelength-sensitive cone photopigment (Kleinschmidt and Harosi, 1992; Wang et al., 1993). This notion was investigated further by exploring the effect of rapid changes in extracellular pH on the dominant time constant in red-sensitive cones. Protons are known to favor the active Meta II form of the photopigment (Parkes and Liebman, 1984), which must be quenched to terminate the response to light. In cones, the photopigment is contained in invaginations of the outer segment plasma membrane and therefore is directly accessible to the external solution (Nilsson, 1964), whereas the other components of the phototransduction cascade are only accessible from the cytoplasm. By briefly exposing the cone outer segment to $0Ca^{2+}/0Na^{+}$ solutions titrated to different pH values with membrane-impermeant buffers (Good et al., 1966), the proton concentration experienced by the photopigment could be manipulated without influencing any other component of the phototransduction cascade while preventing any light-induced changes in outer segment $Ca^{2+}$ concentration.

The approach adopted is illustrated in Fig. 6. The left-hand panels show suction pipette current recordings from four illustrative red-sensitive cones of supersaturating flashes of progressively increasing intensity in $0Ca^{2+}/0Na^{+}$ solutions at pH 6.6, 7.7, 8.5, and 9.0. The outer segment was stepped into $0Ca^{2+}/0Na^{+}$ solution 1 s before each flash and returned to Ringer's solution at 5 or 8 s thereafter; the solution change to the guanidinium-substituted solution was accompanied by a substantial junction current. It can be seen qualitatively that as the pH increased, response recovery was progressively retarded. The right-hand panels plot collected data from several such experiments for the magnitude of the circulating current in darkness in each of these $0Ca^{2+}/0Na^{+}$ solutions of different pH. At pH 6.6, the mean circulating current was markedly depressed, most probably representing proton block of the CNG channels (Picco et al., 1996).

Fig. 7 examines in more detail the effect of these pH changes on the timing of red cone response recovery. In the left-hand panels, the same responses are shown again after subtraction of the junction currents. The time for each response to recover to the criterion level (Fig. 7, dashed lines) was measured to allow the dominant time constant to be determined. The right-hand panels plot collected data from several such experiments at each pH for the time for 25% recovery against the
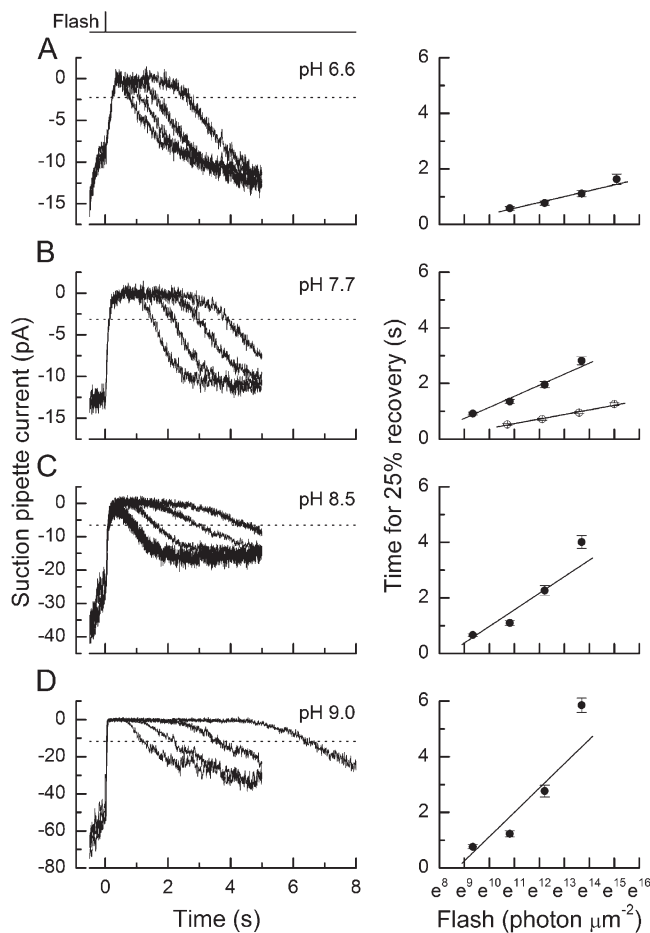
**Figure 7.** Effect of pH on the dominant time constant of red-sensitive cones in the absence of light-induced changes in $Ca^{2+}$ concentration. Flashes of increasing intensity were delivered in $0Ca^{2+}/0Na^+$ solution buffered to pH 6.6, 7.7, 8.5, and 9.0. The left-hand panels show the responses of the four representative cones of Fig. 6 after subtraction of the junction current. The top trace represents flash command timings. Dashed lines represent the 25% criterion recovery level. The closed circles in the right-hand panels plot mean data for the dependence of response duration on flash intensity in $0Ca^{2+}/0Na^+$ solution buffered to the indicated pH values (error bars denote SEM; data were collected from 9 cones at pH 6.6, 49 cones at pH 7.7, 12 cones at pH 8.5, and 16 cones at pH 9.0). The open circles in B represent the corresponding relationship obtained when the flashes were delivered in Ringer's solution at pH 7.7 (mean ± SEM; 17 cells). Regression lines were fitted using a weighted least-squares algorithm; their slopes are plotted as the dominant time constant in Fig. 8 A.

natural logarithm of the flash intensity (Fig. 7, closed circles). The slopes of the regression lines fitted to the data increased monotonically with increasing pH, representing a graded variation in the dominant time constant with external pH when the outer segment $Ca^{2+}$ concentration was held at its dark-adapted value. In addition, Fig. 7 B also includes collected data obtained when the flashes were presented in normal Ringer's solution (open circles), thereby allowing the light-induced fall in $[Ca^{2+}]_i$ to speed the time constant dominating the

recovery of the red-sensitive cone responses (Matthews and Sampath, 2010).

Values for the dominant time constant derived from the slopes of the fitted regression lines are plotted against the corresponding pH in Fig. 8 A. The closed circles represent the time constant obtained at each pH in $0Ca^{2+}/0Na^+$ solution, whereas the open circle denotes the dominant time constant measured when the flashes were delivered in pH 7.7 Ringer's solution. When the outer segment $Ca^{2+}$ concentration was held at its dark-adapted value, the dominant time constant varied in a graded manner with external pH, slowing by a factor of 2.2 upon alkalinisation to pH 9.0 from the normal physiological value of pH 7.7 and shortening by a factor of 1.9 when the external solution was acidified to pH 6.6. At pH values outside this range, cell survival was compromised. For comparison, the dominant time constant at pH 7.7 was accelerated by an even greater factor of 2.4 when the outer segment $Ca^{2+}$ concentration was allowed to fall during the saturated flash response in Ringer's solution (Matthews and Sampath, 2010).

These data are replotted as the corresponding rate constants in Fig. 8 B and have been fitted by a modified Henderson-Hasselbalch equation (solid curve):

$$R = R_{max} \times \left\{ (1 - B) \times \frac{10^{pK-pH}}{1 + 10^{pK-pH}} + B \right\}, \qquad (1)$$

where $R_{max}$ is the maximum value for the rate constant, set equal to its measured value when the saturating flash is delivered in Ringer's solution (Fig. 8 B, open circle and dashed line), $R_{max} \times B$ represents the minimum value for the rate constant at high pH, and $pK$ is the acid dissociation constant for the proton-binding site, which influences the dominant response termination process. The data could be best fitted with a value for $pK$ of 7.1 ± 0.1 and a value for $B$ of 0.22 ± 0.04, which are close to those found for the effects of protons on the equilibrium between the Meta I and II forms of rhodopsin in native rod disk membranes at 20°C (Mahalingam et al., 2008).

Because $[Ca^{2+}]_i$ was maintained at its dark value throughout the flash response, these changes represent the actions of pH on the dominant time constant governing response termination. As the photopigment is the only component of the cone transduction cascade directly exposed to external protons, the simplest interpretation of this result is that protons might act by modifying the proportion of cone photopigment in the active Meta II form that can be quenched. However, an alternative interpretation of this result would be that external pH changes might instead either act at some other nonspecific external site or, alternatively, despite the use of impermeant buffers, result in a sufficient change in cytoplasmic pH to affect subsequent stages of the transduction cascade. To exclude these possibilities,
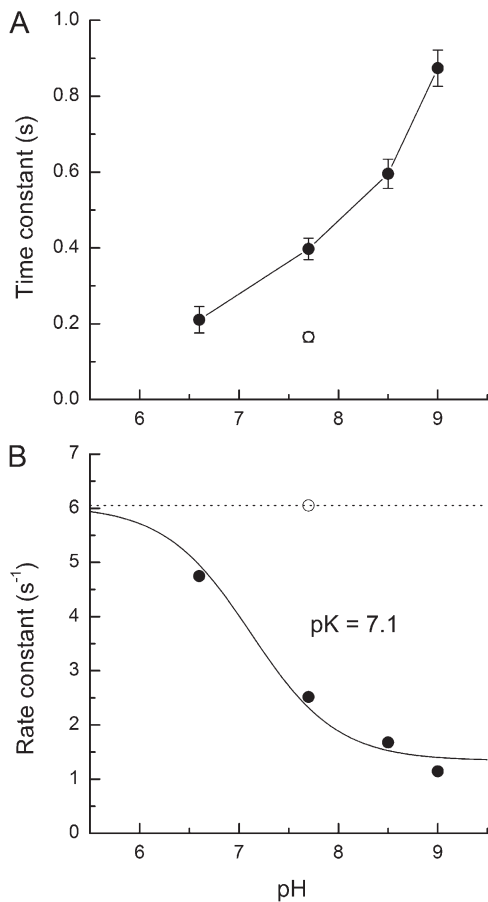
**Figure 8.** Dependence of the dominant time constant on pH in red-sensitive cones. (A) Dominant time constant plotted as a function of pH, obtained from the slopes of the regression lines fitted to the data of the right-hand panels of Fig. 7. Closed circles represent measurements in $0Ca^{2+}/0Na^{+}$ solution; the open circle denotes the dominant time constant when the flash was delivered in Ringer's solution at pH 7.7. Error bars represent SEM calculated by the weighted least-squares fitting algorithm. (B) Corresponding rate constants, calculated as the reciprocal of the dominant time constant, plotted as a function of pH. The closed circles, representing measurements in $0Ca^{2+}/0Na^{+}$ solution, have been fitted with the modified Henderson-Hasselbalch relationship of Eq. 1 using a least-squares algorithm. The fitted curve was constrained to a maximum rate constant ($R_{max}$) corresponding to the dominant time constant measured in Ringer's solution (open circle and dashed line), yielding a $pK$ of 7.1 ± 0.1 and a minimum baseline rate, $B$, at a high pH of 0.22 ± 0.04.

similar experiments were performed in salamander rods, whose photopigment is located in the membrane of the disks, which are topologically separate from the outer segment plasma membrane (Brown et al., 1963) and therefore inaccessible to external protons.

Fig. 9 presents results obtained from rods using a protocol analogous to that used earlier for cones. The left-hand panels show junction-corrected suction pipette current recordings from three illustrative salamander rods of supersaturating flashes of increasing intensity in $0Ca^{2+}/0Na^{+}$ solutions at pH 6.6, 7.6, and 8.6, and the middle panels plot the corresponding times for 25% response

recovery as a function of the natural logarithm of flash intensity in the same three cells. The outer segment was stepped into $0Ca^{2+}/0Na^{+}$ solution 2 s before each flash and returned to Ringer's solution 15 s thereafter to allow for the much slower kinetics of rod phototransduction. Successive exposures evoked a progressive diminution of the circulating current in $0Ca^{2+}/0Na^{+}$ solution, perhaps as the result of the accumulation of guanidinium within the cytoplasm (Fain et al., 1989; Matthews, 1995). To minimize the effect of this decline on the averaged data, flashes were delivered symmetrically in time, with first decreasing and then increasing intensity, and the responses were averaged pairwise across the protocol, whereas the times for 25% recovery were measured individually for each response and averaged at each flash intensity. It can be seen qualitatively from these sample cells that pH had little effect on the timing of rod photoresponse recovery, whereas the slopes of the regression lines fitted to the recovery time data, which represent the dominant time constant for response recovery, were similarly unaffected by pH. The right-hand panels plot collected time constant data from several such experiments at each pH as the means of the slopes of the regression lines fitted to the recovery time data for each rod. It can be seen that external pH changes had no systematic effect on the dominant time constant for rod recovery, and the differences between the means were not significant (one-way ANOVA; F = 1.05, P = 0.37). The lack of effect of both increases and decreases in pH on the rod dominant time constant indicates that the systematic changes that were observed in red-sensitive cones are unlikely to result either from nonspecific actions of external protons or from changes in cytoplasmic pH but instead represent actions of external protons on the exposed cone photopigment.

## DISCUSSION

### $Ca^{2+}$ dependence of response duration is a general feature of amphibian cone phototransduction

This study has investigated the mechanism that regulates termination of the light response in salamander UV-sensitive and blue-sensitive cones. In both of these cone classes, the quenching of the transduction cascade remained sensitive to $Ca^{2+}$ for the entire duration of the bright flash response (Figs. 1–3), in common with red-sensitive cones (Matthews and Sampath, 2010) but in dramatic contrast to the rods of this species (Matthews, 1996; Matthews et al., 2001). In consequence, the time constant that dominates bright flash response recovery is modulated by the dynamic fall in $Ca^{2+}$ concentration that takes place during the light response (Figs. 4 and 5), as in red-sensitive cones (Matthews and Sampath, 2010). Thus, control of the dominant time constant by $Ca^{2+}$ appears to be a common feature of phototransduction in
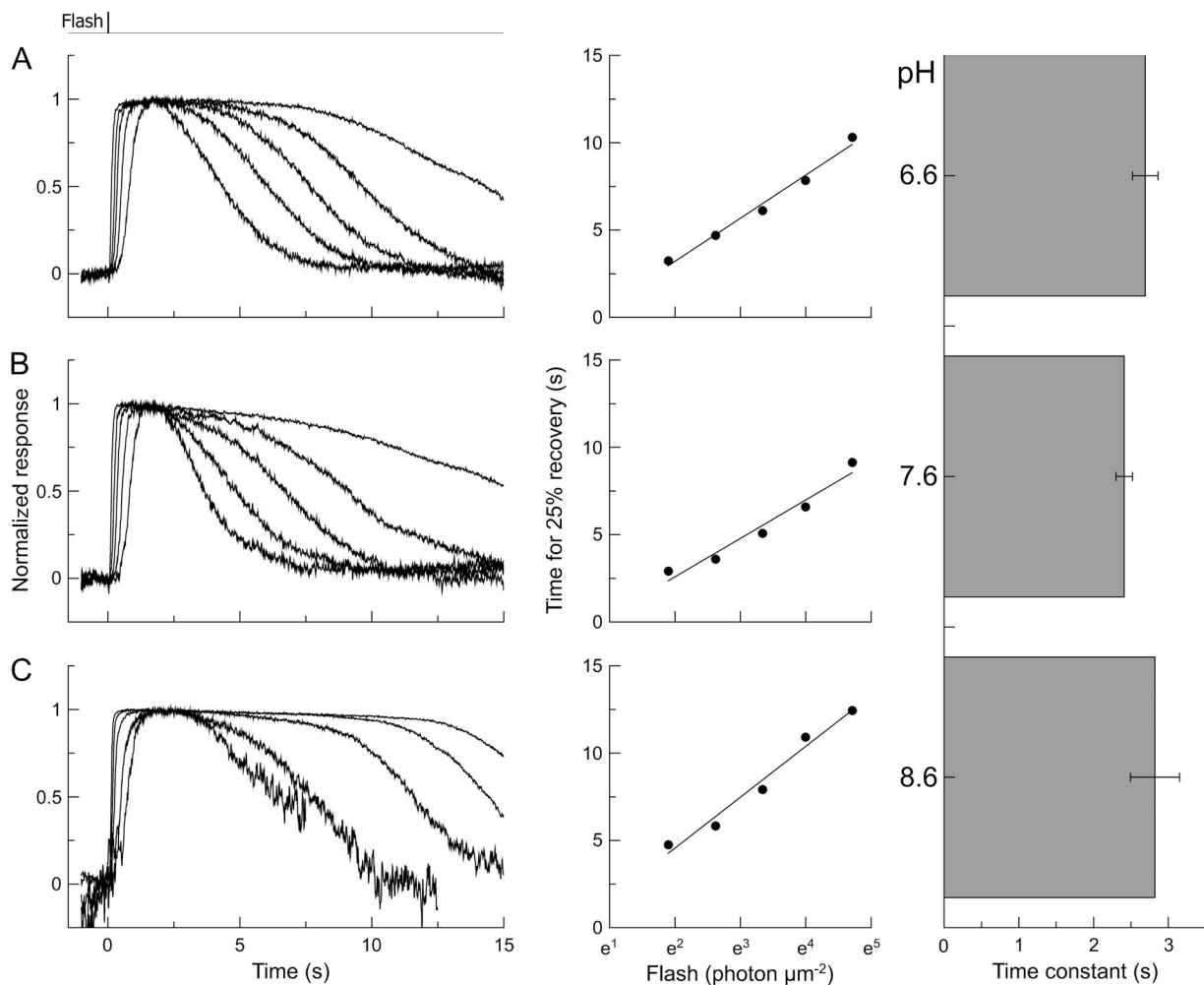
**Figure 9.** Lack of effect of pH on the dominant time constant of salamander rods in the absence of light-induced changes in $Ca^{2+}$ concentration. Flashes of increasing intensity were delivered in $0Ca^{2+}/0Na^+$ solution buffered to pH 6.6, 7.6, and 8.6. Bright flashes at 500 nm were delivered between 6.7 and 111 photons $\mu m^{-2}$ and were presented in a time-symmetrical sequence. The left-hand panels show the responses of three representative rods after subtraction of the junction current. Each trace is the mean of two responses to flashes presented symmetrically in time and has been normalized according to the initial current just before the flash. The top trace represents flash command timings. The closed circles in the middle panels plot the dependence of response duration on flash intensity for each cell; each point is the mean of the values from two symmetrically presented responses. Regression lines were fitted using a least-squares algorithm; their slopes represent the dominant time constant in each cell. The right-hand panel plots collected data from several cells for the mean value of the time constant fitted individually to each cell at pH 6.6 (seven cells), pH 7.6 (eight cells), and pH 8.6 (six cells); error bars represent the SEM. The time constants are not significantly different at the three pH values (one-way ANOVA; F = 1.05, P = 0.37), indicating that external pH has no systematic effect on the dominant time constant in rods.

all three cone classes, exhibiting a more than twofold modulation over the physiological $Ca^{2+}$ concentration range (Figs. 3–5 and 7 B). This is the case despite the considerable differences in sensitivity and response kinetics that exist between the different cone classes in this species (Perry and McNaughton, 1991; Makino and Dodd, 1996). Moreover, the light-induced $Ca^{2+}$ decay in blue-sensitive cones is ~2.2-fold slower than that in red-sensitive cones (Sampath et al., 1999), corresponding well with the ratio of 2.3 between the dominant time constants for response recovery in Ringer's solution in these two cone classes (Figs. 5 B and 7 B). This observation suggests that the dynamics of the decline in $Ca^{2+}$

concentration may be well matched to the absolute magnitude of the dominant time constant in each cone class.

It is important to note, however, that the approach used in this study was designed to investigate the dominant time constant governing the recovery of the responses of cones to saturating flashes. It is thus not clear whether the $Ca^{2+}$ dependence of the cone dominant time constant would necessarily apply for the responses to still higher or lower flash intensities, for which the relative importance of response termination mechanisms may differ. For example, at intensities that cause significant photopigment bleaching, cone response recovery may be dominated by the direct decay of the
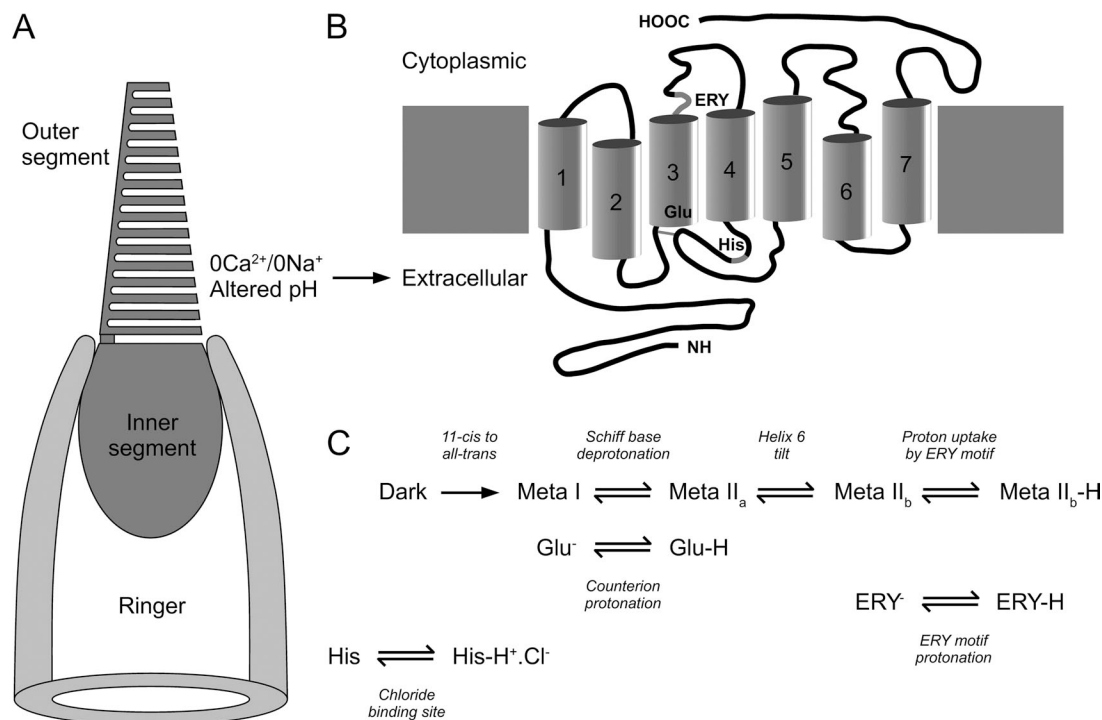
**Figure 10.** Possible sites at which changes in pH might influence the salamander red cone pigment. (A) Recording configuration used to record from red cone photoreceptors. The suction pipette was filled with normal Ringer's solution, whereas the outer segment was briefly exposed to $0Ca^{2+}/0Na^+$ solution of altered pH. Note that the photopigment molecule spans the invaginated cone outer segment membrane, with the consequence that its extracellular (N terminal) face is in contact with the modified bathing solution. (B) Schematic representation of the predicted secondary structure of the salamander red cone pigment (modified from Xu et al., 1998) showing sites known to interact with protons. Numbers denote opsin transmembrane helices. ERY, motif containing a conserved carboxylic acid residue, believed to stabilize the activated Meta IIb form of the pigment (Mahalingam et al., 2008). Glu, conserved glutamine that acts as the counterion for the protonated Schiff base (Jaeger et al., 1994). His, histidine residue conserved in long wavelength cone pigments and believed to constitute the anion-binding site (Wang et al., 1993). (C) Schematic representation of the reactions underlying photopigment activation, modified from the schema for rhodopsin (Mahalingam et al., 2008), indicating the potential involvement of proton binding at the aforementioned sites.

Meta II form of the photopigment (Estevez et al., 2006), whereas it has been suggested that transducin quenching may play the dominant role in cone response recovery at dim flash intensities (Korenbrot, 2012).

### Modulation of the dominant time constant by external pH in red-sensitive cones

The ability of $Ca^{2+}$ to modulate the dominant time constant in red-sensitive cones has been proposed to implicate photopigment quenching as the rate-limiting process in the shutoff of the cone phototransduction cascade (Matthews and Sampath, 2010). In rods, this process involves phosphorylation of the active Meta II form of rhodopsin, which is known to depend on $Ca^{2+}$ (Kawamura, 1993; Chen et al., 1995; Klenchin et al., 1995). In cones, photopigment phosphorylation takes place rapidly after illumination (Tachibanaki et al., 2005), is required for normal response recovery (Rinner et al., 2005) before capping by a cone-specific arrestin (Renninger et al., 2011), and is modulated by $Ca^{2+}$ (Kennedy et al., 2004). In red-sensitive cones, external $Cl^-$ ions bind to the long wavelength-sensitive

cone pigment (Wang et al., 1993), further red-shift its action spectrum (Kleinschmidt and Harosi, 1992), and appear to prolong its catalytic lifetime (Matthews and Sampath, 2010). The shortening of the dominant time constant by withdrawal of external $Cl^-$ thus supports the notion that $Ca^{2+}$-sensitive photopigment quenching dominates red-sensitive cone recovery (Matthews and Sampath, 2010).

In this study, brief changes in external pH in the solution bathing the outer segment were found to modulate the dominant time constant of red-sensitive cones in a graded manner (Figs. 6 and 8). In particular, external acidification accelerated the dominant time constant, indicating that protons must target the rate-limiting process directly (Pugh, 2006). In cones, the surface of the outer segment is invaginated to form sacs whose membrane contains the photopigment (Fig. 10 A), in contrast to the topologically distinct disks of the rod outer segment (Brown et al., 1963). Consequently, the external solution contacts not only the CNG channels and sodium–calcium exchanger, but also the extracellular face of the photopigment, which in a rod would be located

within the disk lumen. Protons are known to block CNG channels (Picco et al., 1996), thereby influencing the magnitude of the dark current (Fig. 6), and to reduce the saturated sodium–calcium exchange current (Hodgkin and Nunn, 1988). However, these actions seem unlikely to have influenced response kinetics in these experiments because $Ca^{2+}$ fluxes across the outer segment membrane were already incapacitated by exposure to $0Ca^{2+}/0Na^+$ solution, thereby rendering both sodium–calcium exchange and the CNG channels irrelevant from the point of view of calcium homeostasis. This conclusion is strengthened by the lack of effect of external pH on the dominant time constant of salamander rods (Fig. 9), in which the photopigment is located in the disk membrane and therefore is not accessible to the external solution and in which rhodopsin quenching is not the process normally dominating response recovery. This result argues against the possibility that changes in dominant time constant in cones might result from non-specific actions of protons at some other external site. Furthermore, it also indicates that such brief changes in external pH are unlikely to have exerted their actions on the cone dominant time constant by altering the pH of the outer segment cytoplasm. Consequently, the changes in cone dominant time constant seem likely to represent actions of protons on the exposed extracellular face of the cone photopigment itself.

Biochemical studies on rhodopsin provide an indication as to how protons might exert these actions on the cone photopigment. Rhodopsin quenching requires phosphorylation of its Meta II form, which is accessible to rhodopsin kinase (Kühn, 1978; Kühn et al., 1982). For any level of rhodopsin kinase activity, the quenching rate of the total activated pool of rhodopsin would be expected to be affected by any manipulation that influences the position of the equilibrium between its Meta I and II forms. An example is provided by the slowed and $Ca^{2+}$-sensitive response recovery observed in rods regenerated with the 9-demethylretinal chromophore (Corson et al., 1994; Matthews et al., 2001), which shifts this equilibrium strongly toward the Meta I form (Meyer et al., 2000; Vogel et al., 2000). Protons have been shown to favor the active Meta II form of rhodopsin in bovine disk membrane suspensions (Parkes and Liebman, 1984). Consequently, rhodopsin quenching might be expected to be more rapid at acidic pH and to be retarded at alkaline pH.

The conformational transition to the active Meta II form of rhodopsin has been shown to involve two protonation switches (Fig. 10 C). The first takes place via an internal proton transfer from the protonated Schiff base to its glutamic acid counterion (E113; Jaeger et al., 1994). Although deprotonation of the Schiff base is often presented as the crucial step in Meta II formation (Longstaff et al., 1986), it appears to be the protonation of the counterion that is necessary for activation (Fahmy et al., 1995) because a Meta II–like photoproduct can be formed even when the Schiff base is also still protonated (Vogel et al., 2001). The second switch involves proton uptake at a highly conserved glutamic acid–binding site (E134) located in the ERY motif at the cytoplasmic face of transmembrane helix 3 (Arnis et al., 1994). It is this second proton switch that is believed to give rise to anomalous pH dependence of the Meta I/Meta II equilibrium (Mahalingam et al., 2008) by stabilizing the active Meta IIb form at acidic pH. In native rod disk membranes, the two protonation switches become partially uncoupled at physiological temperatures, giving rise to an entropy-stabilized but unprotonated Meta IIa state at alkaline pH in which the activating movement of helix 6 has already taken place (Mahalingam et al., 2008; Zaitseva et al., 2010). Comparison of the pH titration curve for the formation of the active Meta II conformation of rhodopsin in native disk membranes (Mahalingam et al., 2008) with the pH dependence of the rate constant for removal of the rate-limiting intermediate in the red cone photoresponse (Fig. 8 B) reveals a striking correspondence.

Homologous sites are present in the salamander red cone pigment (E128 and E149; Xu et al., 1998) for the counterion (Fig. 10 B, Glu) and ERY motif (Fig. 10 B, ERY), respectively. In addition, the anion-binding site of the human medium and long wavelength cone pigments is believed to involve a histidine residue in the extracellular loop between helices 4 and 5 (H197; Wang et al., 1993) that is conserved in the salamander red cone pigment (H196; Fig. 10 B, His; Xu et al., 1998). This has been suggested to form part of a complex Schiff base counterion in its native chloride-liganded state (Kleinschmidt and Harosi, 1992), which would form only after protonation.

So which of these sites for proton binding might contribute to the effect of pH observed in these experiments? Although it is tempting to attribute a role for proton binding to the ERY motif, it seems unlikely that brief exposure of the cone outer segment alone to a $0Ca^{2+}/0Na^+$ solution of modified pH containing an impermeant buffer would have substantially affected the pH of the cytoplasm itself. The ERY motif in the red cone pigment is located just beyond the cytoplasmic face of helix 3 (Xu et al., 1998), and so is not in direct contact with the external solution. Although an influence of extracellular protons on this site cannot be completely excluded because internal water molecules are present within the transmembrane region of the photopigment (Okada et al., 2002), it seems more likely that protons exert their effect through protonation of the counterion (Fig. 10 C, Glu) or the anion-binding site (Fig. 10 C, His), both of which are located on the extracellular face of the red cone pigment (Fig. 10 B), and so either or both might potentially contribute. One potential way of discriminating between these two possibilities would be to extend

these studies in the future to blue- or UV-sensitive cones, which lack the anion-binding site (Kleinschmidt and Harosi, 1992). Nevertheless, the precise site at which protons influence the red cone pigment remains unknown.

## Implications for cone light adaptation

The sensitivity of photoreceptors is reduced during light adaptation to preserve useful signals when the background light intensity rises. Although the overall phototransduction cascade is thought to be similar in both photoreceptor classes, cones do not saturate even in the presence of bright background light (Baylor and Hodgkin, 1974; Matthews et al., 1990; Schneeweis and Schnapf, 1999), whereas rods can only function over a more modest range of intensities. Although photopigment bleaching will contribute to cone desensitization at the highest intensities (Burkhardt, 1994; Paupoo et al., 2000), at dimmer intensities changes in $Ca^{2+}$ concentration seem likely to play a major role. The decline in $Ca^{2+}$ concentration that occurs during the light response serves to accelerate photopigment phosphorylation (Kawamura, 1993; Chen et al., 1995; Kennedy et al., 2004), speed the synthesis of cGMP (Koch and Stryer, 1988), and enhance the cGMP affinity of cGMP-gated channels (Hsu and Molday, 1993; Rebrik et al., 2000). Because most components of the phototransduction cascade exhibit different molecular properties in the two receptor classes, quantitative differences between the individual components and their expression levels seem likely to contribute to the different photoresponse properties (Fu and Yau, 2007). In salamander rod photoreceptors, many of the adaptational changes in photoresponse waveform and sensitivity can be accounted for by the increase in cGMP turnover evoked by steady light (Nikonov et al., 2000), which may be elevated by 10–20-fold over the full adaptational intensity range (Hodgkin and Nunn, 1988; Cornwall and Fain, 1994; Nikonov et al., 2000). In contrast, cyclase rates may be elevated by only 3.5-fold in salamander cones during bright illumination (Cornwall et al., 1995), suggesting that cGMP turnover may play a considerably more modest role in the control of response sensitivity and time course than in rods (Matthews and Sampath, 2010). Furthermore, despite exhibiting more extensive adaptation and a wider calcium dynamic range (Sampath et al., 1999) than rods (Sampath et al., 1998; Woodruff et al., 2002), the responses of mammalian cones appear to be modulated by guanylyl cyclase–activating proteins to a lesser degree than mammalian rods (Sakurai et al., 2011), suggesting that differential modulation of the guanylyl cyclase rate cannot account for the adaptational differences between the two receptor classes. In contrast, visual pigment kinase appears to be modulated to a greater degree in cones than in rods (Arinobu et al., 2010). The demonstration in the present study that dominance of cone bright flash response recovery by $Ca^{2+}$-sensitive pigment quenching is a general feature of amphibian cone phototransduction may provide an additional mechanism by which background light can modulate the sensitivity and time course of the cone photoresponse over its extensive adaptation range.

## REFERENCES

Arinobu, D., S. Tachibanaki, and S. Kawamura. 2010. Larger inhibition of visual pigment kinase in cones than in rods. *J. Neurochem.* 115:259–268. http://dx.doi.org/10.1111/j.1471-4159.2010.06925.x

Arnis, S., K. Fahmy, K.P. Hofmann, and T.P. Sakmar. 1994. A conserved carboxylic acid group mediates light-dependent proton uptake and signaling by rhodopsin. *J. Biol. Chem.* 269:23879–23881.

Arshavsky, V.Y., and M.D. Bownds. 1992. Regulation of deactivation of photoreceptor G protein by its target enzyme and cGMP. *Nature.* 357:416–417. http://dx.doi.org/10.1038/357416a0

Baylor, D.A., and A.L. Hodgkin. 1974. Changes in time scale and sensitivity in turtle photoreceptors. *J. Physiol.* 242:729–758.

Bownds, D., J. Dawes, J. Miller, and M. Stahlman. 1972. Phosphorylation of frog photoreceptor membranes induced by light. *Nat. New Biol.* 237:125–127.

Brown, P.K., I.R. Gibbons, and G. Wald. 1963. The visual cells and visual pigment of the mudpuppy, *Necturus. J. Cell Biol.* 19:79–106. http://dx.doi.org/10.1083/jcb.19.1.79

Burkhardt, D.A. 1994. Light adaptation and photopigment bleaching in cone photoreceptors in situ in the retina of the turtle. *J. Neurosci.* 14:1091–1105.

Burns, M.E., and D.A. Baylor. 2001. Activation, deactivation, and adaptation in vertebrate photoreceptor cells. *Annu. Rev. Neurosci.* 24:779–805. http://dx.doi.org/10.1146/annurev.neuro.24.1.779

Burns, M.E., and E.N. Pugh Jr. 2010. Lessons from photoreceptors: turning off g-protein signaling in living cells. *Physiology (Bethesda).* 25:72–84. http://dx.doi.org/10.1152/physiol.00001.2010

Chen, C.-K., J. Inglese, R.J. Lefkowitz, and J.B. Hurley. 1995. Ca(2+)-dependent interaction of recoverin with rhodopsin kinase. *J. Biol. Chem.* 270:18060–18066. http://dx.doi.org/10.1074/jbc.270.30.18060

Cornwall, M.C., and G.L. Fain. 1994. Bleached pigment activates transduction in isolated rods of the salamander retina. *J. Physiol.* 480:261–279.

Cornwall, M.C., H.R. Matthews, R.K. Crouch, and G.L. Fain. 1995. Bleached pigment activates transduction in salamander cones. *J. Gen. Physiol.* 106:543–557. http://dx.doi.org/10.1085/jgp.106.3.543

Corson, D.W., M.C. Cornwall, and D.R. Pepperberg. 1994. Evidence for the prolonged photoactivated lifetime of an analogue visual pigment containing 11-cis 9-desmethylretinal. *Vis. Neurosci.* 11:91–98. http://dx.doi.org/10.1017/S0952523800011135

Doan, T., A.W. Azevedo, J.B. Hurley, and F. Rieke. 2009. Arrestin competition influences the kinetics and variability of the single-photon responses of mammalian rod photoreceptors. *J. Neurosci.* 29:11867–11879. http://dx.doi.org/10.1523/JNEUROSCI.0819-09.2009

Estevez, M.E., P. Ala-Laurila, R.K. Crouch, and M.C. Cornwall. 2006. Turning cones off: the role of the 9-methyl group of retinal in red cones. *J. Gen. Physiol.* 128:671–685. http://dx.doi.org/10.1085/jgp.200609630

Fahmy, K., F. Siebert, and T.P. Sakmar. 1995. Photoactivated state of rhodopsin and how it can form. *Biophys. Chem.* 56:171–181. http://dx.doi.org/10.1016/0301-4622(95)00030-2

Fain, G.L., T.D. Lamb, H.R. Matthews, and R.L. Murphy. 1989. Cytoplasmic calcium as the messenger for light adaptation in salamander rods. *J. Physiol.* 416:215–243.

Fain, G.L., H.R. Matthews, M.C. Cornwall, and Y. Koutalos. 2001. Adaptation in vertebrate photoreceptors. *Physiol. Rev.* 81:117–151.

Fu, Y., and K.-W. Yau. 2007. Phototransduction in mouse rods and cones. *Pflugers Arch.* 454:805–819. http://dx.doi.org/10.1007/s00424-006-0194-y

Good, N.E., G.D. Winget, W. Winter, T.N. Connolly, S. Izawa, and R.M. Singh. 1966. Hydrogen ion buffers for biological research. *Biochemistry.* 5:467–477. http://dx.doi.org/10.1021/bi00866a011

Gross, O.P., and M.E. Burns. 2010. Control of rhodopsin's active lifetime by arrestin-1 expression in mammalian rods. *J. Neurosci.* 30:3450–3457. http://dx.doi.org/10.1523/JNEUROSCI.5391-09.2010

Hárosi, F.I. 1975. Absorption spectra and linear dichroism of some amphibian photoreceptors. *J. Gen. Physiol.* 66:357–382. http://dx.doi.org/10.1085/jgp.66.3.357

Hodgkin, A.L., and B.J. Nunn. 1988. Control of light-sensitive current in salamander rods. *J. Physiol.* 403:439–471.

Hsu, Y.-T., and R.S. Molday. 1993. Modulation of the cGMP-gated channel of rod photoreceptor cells by calmodulin. *Nature.* 361:76–79. http://dx.doi.org/10.1038/361076a0

Jaeger, F., K. Fahmy, T.P. Sakmar, and F. Siebert. 1994. Identification of glutamic acid 113 as the Schiff base proton acceptor in the metarhodopsin II photointermediate of rhodopsin. *Biochemistry.* 33:10878–10882. http://dx.doi.org/10.1021/bi00202a005

Kawamura, S. 1993. Rhodopsin phosphorylation as a mechanism of cyclic GMP phosphodiesterase regulation by S-modulin. *Nature.* 362:855–857. http://dx.doi.org/10.1038/362855a0

Kennedy, M.J., F.A. Dunn, and J.B. Hurley. 2004. Visual pigment phosphorylation but not transducin translocation can contribute to light adaptation in zebrafish cones. *Neuron.* 41:915–928. http://dx.doi.org/10.1016/S0896-6273(04)00086-8

Kleinschmidt, J., and F.I. Harosi. 1992. Anion sensitivity and spectral tuning of cone visual pigments in situ. *Proc. Natl. Acad. Sci. USA.* 89:9181–9185. http://dx.doi.org/10.1073/pnas.89.19.9181

Klenchin, V.A., P.D. Calvert, and M.D. Bownds. 1995. Inhibition of rhodopsin kinase by recoverin. Further evidence for a negative feedback system in phototransduction. *J. Biol. Chem.* 270:16147–16152.

Koch, K.-W., and L. Stryer. 1988. Highly cooperative feedback control of retinal rod guanylate cyclase by calcium ions. *Nature.* 334:64–66. http://dx.doi.org/10.1038/334064a0

Korenbrot, J.I. 2012. Speed, adaptation, and stability of the response to light in cone photoreceptors: the functional role of Ca-dependent modulation of ligand sensitivity in cGMP-gated ion channels. *J. Gen. Physiol.* 139:31–56. http://dx.doi.org/10.1085/jgp.201110654

Krispel, C.M., D. Chen, N. Melling, Y.-J. Chen, K.A. Martemyanov, N. Quillinan, V.Y. Arshavsky, T.G. Wensel, C.-K. Chen, and M.E. Burns. 2006. RGS expression rate-limits recovery of rod photoresponses. *Neuron.* 51:409–416. http://dx.doi.org/10.1016/j.neuron.2006.07.010

Kühn, H. 1978. Light-regulated binding of rhodopsin kinase and other proteins to cattle photoreceptor membranes. *Biochemistry.* 17:4389–4395. http://dx.doi.org/10.1021/bi00614a006

Kühn, H., and W.J. Dreyer. 1972. Light dependent phosphorylation of rhodopsin by ATP. *FEBS Lett.* 20:1–6. http://dx.doi.org/10.1016/0014-5793(72)80002-4

Kühn, H., O. Mommertz, and P.A. Hargrave. 1982. Light-dependent conformational change at rhodopsin's cytoplasmic surface detected by increased susceptibility to proteolysis. *Biochim. Biophys. Acta.* 679:95–100. http://dx.doi.org/10.1016/0005-2728(82)90259-6

Kühn, H., S.W. Hall, and U. Wilden. 1984. Light-induced binding of 48-kDa protein to photoreceptor membranes is highly enhanced by phosphorylation of rhodopsin. *FEBS Lett.* 176:473–478. http://dx.doi.org/10.1016/0014-5793(84)81221-1

Lamb, T.D., and E.N. Pugh Jr. 2006. Phototransduction, dark adaptation, and rhodopsin regeneration. The proctor lecture. *Invest. Ophthalmol. Vis. Sci.* 47:5138–5152. http://dx.doi.org/10.1167/iovs.06-0849

Longstaff, C., R.D. Calhoon, and R.R. Rando. 1986. Deprotonation of the Schiff base of rhodopsin is obligate in the activation of the G protein. *Proc. Natl. Acad. Sci. USA.* 83:4209–4213. http://dx.doi.org/10.1073/pnas.83.12.4209

Lyubarsky, A., S. Nikonov, and E.N. Pugh Jr. 1996. The kinetics of inactivation of the rod phototransduction cascade with constant $Ca^{2+}_i$. *J. Gen. Physiol.* 107:19–34. http://dx.doi.org/10.1085/jgp.107.1.19

Mahalingam, M., K. Martínez-Mayorga, M.F. Brown, and R. Vogel. 2008. Two protonation switches control rhodopsin activation in membranes. *Proc. Natl. Acad. Sci. USA.* 105:17795–17800. http://dx.doi.org/10.1073/pnas.0804541105

Makino, C.L., and R.L. Dodd. 1996. Multiple visual pigments in a photoreceptor of the salamander retina. *J. Gen. Physiol.* 108:27–34. http://dx.doi.org/10.1085/jgp.108.1.27

Matthews, H.R. 1995. Effects of lowered cytoplasmic calcium concentration and light on the responses of salamander rod photoreceptors. *J. Physiol.* 484:267–286.

Matthews, H.R. 1996. Static and dynamic actions of cytoplasmic $Ca^{2+}$ in the adaptation of responses to saturating flashes in salamander rods. *J. Physiol.* 490:1–15.

Matthews, H.R. 1997. Actions of $Ca^{2+}$ on an early stage in phototransduction revealed by the dynamic fall in $Ca^{2+}$ concentration during the bright flash response. *J. Gen. Physiol.* 109:141–146. http://dx.doi.org/10.1085/jgp.109.2.141

Matthews, H.R., and G.L. Fain. 2003. The effect of light on outer segment calcium in salamander rods. *J. Physiol.* 552:763–776. http://dx.doi.org/10.1113/jphysiol.2003.050724

Matthews, H.R., and A.P. Sampath. 2010. Photopigment quenching is $Ca^{2+}$ dependent and controls response duration in salamander L-cone photoreceptors. *J. Gen. Physiol.* 135:355–366. http://dx.doi.org/10.1085/jgp.200910394

Matthews, H.R., R.L. Murphy, G.L. Fain, and T.D. Lamb. 1988. Photoreceptor light adaptation is mediated by cytoplasmic calcium concentration. *Nature.* 334:67–69. http://dx.doi.org/10.1038/334067a0

Matthews, H.R., G.L. Fain, R.L. Murphy, and T.D. Lamb. 1990. Light adaptation in cone photoreceptors of the salamander: a role for cytoplasmic calcium. *J. Physiol.* 420:447–469.

Matthews, H.R., M.C. Cornwall, and R.K. Crouch. 2001. Prolongation of actions of $Ca^{2+}$ early in phototransduction by 9-demethylretinal. *J. Gen. Physiol.* 118:377–390. http://dx.doi.org/10.1085/jgp.118.4.377

Meyer, C.K., M. Böhme, A. Ockenfels, W. Gärtner, K.P. Hofmann, and O.P. Ernst. 2000. Signaling states of rhodopsin. Retinal provides a scaffold for activating proton transfer switches. *J. Biol. Chem.* 275:19713–19718. http://dx.doi.org/10.1074/jbc.M000603200

Nakatani, K., and K.-W. Yau. 1988. Calcium and light adaptation in retinal rods and cones. *Nature.* 334:69–71. http://dx.doi.org/10.1038/334069a0

Nikonov, S., N. Engheta, and E.N. Pugh Jr. 1998. Kinetics of recovery of the dark-adapted salamander rod photoresponse. *J. Gen. Physiol.* 111:7–37. http://dx.doi.org/10.1085/jgp.111.1.7

Nikonov, S., T.D. Lamb, and E.N. Pugh Jr. 2000. The role of steady phosphodiesterase activity in the kinetics and sensitivity of the light-adapted salamander rod photoresponse. *J. Gen. Physiol.* 116:795–824. http://dx.doi.org/10.1085/jgp.116.6.795

Nilsson, S.E. 1964. An electron microscopic classification of the retinal receptors of the leopard frog (*Rana pipiens*). *J. Ultrastruct. Res.* 10:390–416. http://dx.doi.org/10.1016/S0022-5320(64)80018-6

Okada, T., Y. Fujiyoshi, M. Silow, J. Navarro, E.M. Landau, and Y. Shichida. 2002. Functional role of internal water molecules in rhodopsin revealed by X-ray crystallography. *Proc. Natl. Acad. Sci. USA.* 99:5982–5987. http://dx.doi.org/10.1073/pnas.082666399

Parkes, J.H., and P.A. Liebman. 1984. Temperature and pH dependence of the metarhodopsin I-metarhodopsin II kinetics and equilibria in bovine rod disk membrane suspensions. *Biochemistry.* 23:5054–5061. http://dx.doi.org/10.1021/bi00316a035

Paupoo, A.A., O.A. Mahroo, C. Friedburg, and T.D. Lamb. 2000. Human cone photoreceptor responses measured by the electro-retinogram *a*-wave during and after exposure to intense illumination. *J. Physiol.* 529:469–482. http://dx.doi.org/10.1111/j.1469-7793.2000.00469.x

Pepperberg, D.R., M.C. Cornwall, M. Kahlert, K.P. Hofmann, J. Jin, G.J. Jones, and H. Ripps. 1992. Light-dependent delay in the falling phase of the retinal rod photoresponse. *Vis. Neurosci.* 8:9–18. http://dx.doi.org/10.1017/S0952523800006441

Perry, R.J., and P.A. McNaughton. 1991. Response properties of cones from the retina of the tiger salamander. *J. Physiol.* 433:561–587.

Picco, C., C. Sanfilippo, P. Gavazzo, and A. Menini. 1996. Modulation by internal protons of native cyclic nucleotide-gated channels from retinal rods. *J. Gen. Physiol.* 108:265–276. http://dx.doi.org/10.1085/jgp.108.4.265

Pugh, E.N. Jr. 2006. RGS expression level precisely regulates the duration of rod photoresponses. *Neuron.* 51:391–393. http://dx.doi.org/10.1016/j.neuron.2006.08.002

Rebrik, T.I., E.A. Kotelnikova, and J.I. Korenbrot. 2000. Time course and Ca$^{2+}$ dependence of sensitivity modulation in cyclic GMP-gated currents of intact cone photoreceptors. *J. Gen. Physiol.* 116:521–534. http://dx.doi.org/10.1085/jgp.116.4.521

Renninger, S.L., M. Gesemann, and S.C.F. Neuhauss. 2011. Cone arrestin confers cone vision of high temporal resolution in zebrafish larvae. *Eur. J. Neurosci.* 33:658–667. http://dx.doi.org/10.1111/j.1460-9568.2010.07574.x

Rinner, O., Y.V. Makhankov, O. Biehlmaier, and S.C.F. Neuhauss. 2005. Knockdown of cone-specific kinase GRK7 in larval zebrafish leads to impaired cone response recovery and delayed dark adaptation. *Neuron.* 47:231–242. http://dx.doi.org/10.1016/j.neuron.2005.06.010

Sagoo, M.S., and L. Lagnado. 1997. G-protein deactivation is rate-limiting for shut-off of the phototransduction cascade. *Nature.* 389:392–395. http://dx.doi.org/10.1038/38750

Sakurai, K., J. Chen, and V.J. Kefalov. 2011. Role of guanylyl cyclase modulation in mouse cone phototransduction. *J. Neurosci.* 31:7991–8000. http://dx.doi.org/10.1523/JNEUROSCI.6650-10.2011

Sampath, A.P., H.R. Matthews, M.C. Cornwall, and G.L. Fain. 1998. Bleached pigment produces a maintained decrease in outer segment Ca$^{2+}$ in salamander rods. *J. Gen. Physiol.* 111:53–64. http://dx.doi.org/10.1085/jgp.111.1.53

Sampath, A.P., H.R. Matthews, M.C. Cornwall, J. Bandarchi, and G.L. Fain. 1999. Light-dependent changes in outer segment free-Ca$^{2+}$ concentration in salamander cone photoreceptors. *J. Gen. Physiol.* 113:267–277. http://dx.doi.org/10.1085/jgp.113.2.267

Schneeweis, D.M., and J.L. Schnapf. 1999. The photovoltage of macaque cone photoreceptors: adaptation, noise, and kinetics. *J. Neurosci.* 19:1203–1216.

Tachibanaki, S., D. Arinobu, Y. Shimauchi-Matsukawa, S. Tsushima, and S. Kawamura. 2005. Highly effective phosphorylation by G protein-coupled receptor kinase 7 of light-activated visual pigment in cones. *Proc. Natl. Acad. Sci. USA.* 102:9329–9334. http://dx.doi.org/10.1073/pnas.0501875102

Vogel, R., G.-B. Fan, M. Sheves, and F. Siebert. 2000. The molecular origin of the inhibition of transducin activation in rhodopsin lacking the 9-methyl group of the retinal chromophore: a UV-Vis and FTIR spectroscopic study. *Biochemistry.* 39:8895–8908. http://dx.doi.org/10.1021/bi000852b

Vogel, R., G.-B. Fan, F. Siebert, and M. Sheves. 2001. Anions stabilize a metarhodopsin II-like photoproduct with a protonated Schiff base. *Biochemistry.* 40:13342–13352. http://dx.doi.org/10.1021/bi0113667

Wang, Z., A.B. Asenjo, and D.D. Oprian. 1993. Identification of the Cl$^-$-binding site in the human red and green color vision pigments. *Biochemistry.* 32:2125–2130. http://dx.doi.org/10.1021/bi00060a001

Woodruff, M.L., A.P. Sampath, H.R. Matthews, N.V. Krasnoperova, J. Lem, and G.L. Fain. 2002. Measurement of cytoplasmic calcium concentration in the rods of wild-type and transducin knock-out mice. *J. Physiol.* 542:843–854. http://dx.doi.org/10.1113/jphysiol.2001.013987

Xu, L., E.S. Hazard III, D.K. Lockman, R.K. Crouch, and J. Ma. 1998. Molecular cloning of the salamander red and blue cone visual pigments. *Mol. Vis.* 4:10.

Yau, K.W., and K. Nakatani. 1985. Light-induced reduction of cytoplasmic free calcium in retinal rod outer segment. *Nature.* 313:579–582. http://dx.doi.org/10.1038/313579a0

Zaitseva, E., M.F. Brown, and R. Vogel. 2010. Sequential rearrangement of interhelical networks upon rhodopsin activation in membranes: the Meta II(a) conformational substate. *J. Am. Chem. Soc.* 132:4815–4821. http://dx.doi.org/10.1021/ja910317a